Smart Structures and Systems, *Vol. 26, No. 3 (2020) 345-360*
DOI: https://doi.org/10.12989/sss.2020.26.3.345

A hybrid identification method on butterfly optimization and differential evolution algorithm

Hongyuan Zhou [1], Guangcai Zhang [1], Xiaojuan Wang*[1], Pinghe Ni [1] and Jian Zhang [2]

[1] *Key Laboratory of Urban Security and Disaster Engineering of Ministry of Education, Beijing University of Technology, Beijing 100124, China*
[2] *Faculty of Civil Engineering and Mechanics, Jiangsu University, Zhenjiang 212013, China*

(*Received January 22, 2020, Revised June 2, 2020, Accepted June 14, 2020*)

Abstract. Modern swarm intelligence heuristic search methods are widely applied in the field of structural health monitoring due to their advantages of excellent global search capacity, loose requirement of initial guess and ease of computational implementation etc. To this end, a hybrid strategy is proposed based on butterfly optimization algorithm (BOA) and differential evolution (DE) with purpose of effective combination of their merits. In the proposed identification strategy, two improvements including mutation and crossover operations of DE, and dynamic adaptive operators are introduced into original BOA to reduce the risk to be trapped in local optimum and increase global search capability. The performance of the proposed algorithm, hybrid butterfly optimization and differential evolution algorithm (HBODEA) is evaluated by two numerical examples of a simply supported beam and a 37-bar truss structure, as well as an experimental test of 8-story shear-type steel frame structure in the laboratory. Compared with BOA and DE, the numerical and experimental results show that the proposed HBODEA is more robust to detect the reduction of stiffness with limited sensors and contaminated measurements. In addition, the effect of search space, two dynamic operators, population size on identification accuracy and efficiency of the proposed identification strategy are further investigated.

Keywords: butterfly optimization algorithm; differential evolution; hybrid algorithm; structural damage detection; parameter identification; dynamic adaptive operator

1. Introduction

Civil structures may inevitably accumulate damage during their service period, due to environmental loads, material degradation, fatigue and corrosion, etc. If the gradually developed structural damage is not accurately detected in time, this potential threat may affect performance of structures, or even lead to the collapse of overall structure, resulting in catastrophically unaffordable tragedy. Therefore, to detect damage at early stage to avoid unexpected failures, considerable number of structural health monitoring and damage detection techniques have been proposed to detect, locate, and quantify the damage over the past two decades. In general, structural parameter identification and damage detection methods can be classified into two categories: frequency domain methods and time domain methods (Lu and Gao 2005). The former frequency domain methods utilized the modal information, such as natural frequencies (Maity and Tripathy 2005, Liang *et al*. 2019), model shapes (He and Zhou 2019), model strain energy (Dewangan *et al.* 2020), mode shapes curvatures (Cao *et al.* 2014), model flexibility (Liu *et al.* 2018, Wickramasinghe *et al.* 2020) etc. to identify structural physical parameters, such as stiffness, mass and damping ratio etc. Although fruitful research results have been achieved on their practical application, these frequency domain methods remain the drawbacks that the low modes of modal information are less sensitive to local minor damage and high mode modal responses are difficult to be acquired.

For the latter time domain methods, it is straightforward to identify structural parameters utilizing measured structural dynamic responses with some sensors, and it can be easily treated as an optimization problem with objective function of minimizing the difference between estimated and measured structural responses. Many traditional optimization methods for structural parameter identification were proposed, e.g., a sensitivity-based damage detection methods (Mirzaee *et al.* 2015), an enhanced response sensitivity approach (Lu and Wang 2017), a modified extended Kalman filter method (Lee and Yun 2008), an adaptive extended Kalman filter (AEKF) approach (Zhou *et al.* 2008), a unscented Kalman filter (UKF) method (Chatzi and Fuggini 2015), an iterative method combining biconjugate gradient method and reduction of search space (Sotoudehnia *et al.* 2019), an adaptive quadratic sum-squares error method (Yang *et al.* 2009). For most traditional methods, a good initial value and gradient information are usually required, otherwise the accuracy of identification results are difficult to be guaranteed.

Compared with these traditional methods, some non-classical methods such as neural networks (Padil *et al.* 2020, Ding *et al.* 2020) and swarm intelligent heuristic algorithms which have the advantages of strong global search capacity, loose initial guess and ease of

*Corresponding author, Ph.D., Associate Professor,
E-mail: xiaojuanwang@bjut.edu.cn

ISSN: 1738-1584 (Print), 1738-1991 (Online)

implementation, becoming one of current research hotspots. Plenty of modern heuristic intelligent algorithms have been proposed and widely applied for structural parameter identification, such as the genetic algorithm (Kim *et al.* 2007), the particle swarm optimization algorithm (Zhang *et al.* 2016), the differential evolutionary (DE) algorithm (Vo-Duy *et al*. 2016), artificial bee colony (Ding *et al*. 2016), the firefly algorithm (Pan *et al.* 2016), wolf optimization algorithm (Yi *et al.* 2016), dolphin echolocation algorithm (Kaveh *et al.* 2016), etc. In recent years, a new nature-inspired swarm intelligent algorithm by mimicking the foraging and mating behavior of butterflies (Arora and Singh 2015), named butterfly optimization algorithm (BOA), has been proposed to solve complex optimization problems. It is found that the mechanism to propagate fragrance information is the main characteristic of BOA and plays an important role in its performance. Some relevant researches have been reported in recent years. Arora and Singh (2017b) applied BOA to locate the position of the sensor nodes in wireless sensor networks, presenting the better accuracy and efficiency than firefly algorithm and particle swarm optimization. To further examine the performance of BOA compared with more other heuristic search methods, a set of 30 benchmark test functions and some realistic engineering problems, such as spring design, welded beam design and gear train design were taken as targets, and BOA yielded best optimization solution compared with genetic algorithm, DE, artificial bee colony, firefly algorithm, particle swarm optimization, and cuckoo search (Arora and Singh 2018). Although BOA demonstrated strong global and local search ability in the benchmark test problems, it still faces the problems of slow convergence and the unneglected threat of falling into local optimum. To further improve the performance of BOA, Li *et al.* (2019) proposed the cross-entropy method embedded into the BOA to achieve a tradeoff between global exploration and local exploitation. Singh and Anand (2019) developed an adaptive butterfly optimization algorithm by making operator vary with iteration, achieving better performance than original BOA. Besides further exploring the merits of BOA to improve its performance, hybrid algorithm provides an alternative with concept of effectively combing the advantages of different algorithms due to considerable number of successful applications, such as a hybrid genetic algorithm and particle swarm method (Vosoughi 2015), immune monkey algorithm (Yi *et al.* 2015), A hybrid ant lion optimizer (Chen and Yu 2019), particle swarm method hybrid with cuckoo search (Huang *et al.* 2019), a modified bat algorithm in conjunction with the DE (Yildizdan and Baykan 2020) etc. Some researchers also have tried to incorporate other optimization methods to further improve the performance of BOA, such as a hybrid BOA and artificial bee colony algorithm (Arora and Singh 2017a), a hybrid BOA and learning automata algorithm (Arora and Anand 2018).

In one aspect, some research results showed that effective incorporation with other optimization methods is able to significantly improve the performance of BOA. In other aspect, DE is a simple but powerful global optimization algorithm, and it has received much attention and application due to its excellent global optimization ability. For example, Tang *et al.* (2008) utilized DE to identify structural parameters including mass, stiffness, and damping. Seyedpoor *et al.* (2018b) proposed a multi-stage improved differential evolution algorithm (MSIDEA) to detect multiple damage of structural system. The excellent global search ability of DE owns to its embedded crossover and mutation operators, which allows DE explore more potential candidates. Therefore, in this paper, a hybrid butterfly optimization and differential evolution algorithm (HBODEA), introducing the mutation and crossover of DE into BOA, is proposed to improve the global search capability of BOA. In the proposed hybrid algorithm, the strong local exploitation capability of BOA and global exploration capability of DE are effectively incorporated to improve the convergence rate as well as reduce the risk to be trapped in local optimum. For comparison study, three different optimization methods, namely BOA, DE and HBODEA, are applied to identify the single or multiple damage of structures subjected to unknown white noise excitations numerically (a simply supported beam and truss) and experimentally (8-floor steel frame). The numerical and experimental results show that the proposed HBODEA is more competitive and robust to accurately detect structural damage. Subsequently, the effect of search space, two dynamic operators, population size on identification accuracy and efficiency are further investigated.

2. Problem formulation

2.1 Structural damage model

The equation of motion for a damped linear structural system can be stated as Eq. (1)

$$M\ddot{u}(t) + C\dot{u}(t) + Ku(t) = F(t) \tag{1}$$

where $\boldsymbol{M}$, $\boldsymbol{C}$, and $\boldsymbol{K}$ denote mass, damping and stiffness matrices of the structural system, respectively; $\ddot{u}(t)$, $\dot{u}(t)$ and $u(t)$ represent acceleration, velocity and displacement vectors, respectively; $\boldsymbol{F}(t)$ is the time-dependent excitation force applied to the structure. The damping can be modeled as Rayleigh damping and 5% critical damping is assumed for the first two modes in the numerical examples of the present study.

In general, structural local damage is assumed only in the form of reduction of structural elemental stiffness, and damage is not accompanied by a change in mass (Kang *et al.* 2012, Huo *et al.* 2016, Ding *et al*. 2019). The damaged global stiffness matrix K_d can be expressed as Eq. (2)

$$K_d = \sum_{i=1}^{n} (1 - a_i)\, K_i^e \tag{2}$$

where n stands for total number of structural elements; K_i^e represents i-th undamaged element stiffness matrix, α_i is the corresponding damage index, e.g., $\alpha_i = 0$ implies that there is no damage in structure, and $\alpha_i = 1$ stands for the structure

gets completely damaged. Therefore, the problem of structural damage identification can be concluded to identify damage index α.

2.2 Objective function

The basic idea of vibration-based structural damage identification is that damage in the structure would change its physical properties such as mass and stiffness etc., leading to variation of its dynamic responses. Therefore, it is feasible to inversely identify structural damages with its dynamic responses (displacement, velocity, acceleration) measured by some sensors. In this paper, since acceleration are easy and economical to be accurately acquired in practice, they are applied in the objective function for evaluation of possible candidates. The objective function is defined by minimize the difference between the measured response $\boldsymbol{R}_{mea}$ and the calculated response $\boldsymbol{R}_{cal}$ as below (Wang *et al.* 2020)

$$fitness = \frac{1}{c + \sum_{i=1}^{M}\sum_{j=1}^{L}\frac{|R_{cal}(i,j)-R_{mea}(i,j)|^2}{E\left(R_{mea}^2(i)\right)}} \tag{3}$$

where L and M are the number of data points and measurements; $E(R_{mea}^2(i)) = \sum_{n=1}^{L} R_{mea}^2(i)/L$ represents the mean squared value of i-th measurements. Constant c is chosen to have the same order of normalized summed square error (the second term in the denominator of the fitness function).

It is noted that structural parameter identification is a typical type of inverse problems with considerable number of unknowns and limited measurements, which may introduce huge difficulties to some traditional optimization methods, leading to unsatisfactory identification results, or even local optima. In contrast, considerable number of modern swarm intelligence heuristic search methods have demonstrated their powerful global search capacity, and they would facilitate structural parameter identification, a complex optimization problem, for accurate and efficient identification results.

3. The algorithm for structural damage identification

3.1 Butterfly optimization algorithm

BOA is a recently developed swarm intelligent heuristic algorithm by mimicking foraging behaviors of butterflies. It is found that butterflies can utilize smell to sense chemoreceptors which are distributed over their body to determine the potential location of food or mating partner (Blair and Launer 1997, Raguso 2008). In BOA, the location of butterflies can be known as feasible solutions, meanwhile butterflies will emit fragrance associated with their fitness. More specifically, the fitness will vary if butterflies move from one position to another in search domain, and fragrance spreads with movement of butterflies simultaneously, thus each butterfly can sense fragrance produced by other butterflies and move toward to the best butterfly location.

Similar with other population-based algorithm, initial population of butterflies x_{ij} is produced as

$$x_{ij} = x_{ij}^{l} + r_{ij} \times \left(x_{ij}^{u} - x_{ij}^{l}\right) \tag{4}$$

where x_{ij}^{u} and x_{ij}^{l} denote the upper and lower boundary of the search domain; r_{ij} is a random number uniformly distributed over the interval [0, 1].

Modulation fragrance to guide the search is the main characteristic of BOA, which is dependent on three vital parameters, namely sensory modality (C), stimulus intensity (I) and power exponent (A). The fragrance (f) perceived by butterflies is calculated as a function of the stimulus intensity (Arora and Singh 2018) as follows

$$f_i = CI^A \tag{5}$$

where f_i stands for the magnitude of fragrance smelt by the i-th butterfly; C denotes the sensory modality taken from [0, ∞], determining the speed of convergence; I is the magnitude of stimulus intensity, correlated with the encoded objective function; A is the power exponent influencing reduction of fragrance within the range of [0, 1]. A = 1 means no loss of fragrance, in other words, the amount of fragrance produced by a butterfly equals to that perceived by other butterflies. On the contrary, A = 0 implies all fragrance lost, so it is impossible for any butterflies to sense the fragrance. A butterfly will move toward to the best butterfly location, if it can sense fragrance emitted by the best butterfly, thus the new potential solution is generated by

$$x_i^{G+1} = x_i^G + r^2 \times (g_i^* - x_i^G) \times f_i \tag{6}$$

where x_i^{G+1} and x_i^G are the solutions of the i-th butterfly in iteration of G+1 and G, respectively; g_i^* stands for the best-so-far solution among all iterations; r is a random number uniformly distributed over the interval [0, 1]; f_i represents magnitude of fragrance smelt by the i-th butterfly.

A butterfly will take a random walk, if it cannot sense fragrance emitted by any other butterflies. The new candidate will be generated by randomly choosing two different butterflies from the solution space, which would significantly improve the exploration ability of BOA

$$x_i^{G+1} = x_i^G + r^2 \times \left(x_j^G - x_k^G\right) \times f_i \tag{7}$$

where x_j^G and x_k^G are the solutions of j-th and k-th butterflies in iteration of G, respectively.

It is clear that Eqs. (6)-(7) guide the possible candidates approach to the location of the best butterfly and explore the new potential solutions, corresponding to the local and global search in BOA, respectively. To balance the local and global search, a switch probability parameter P taken from [0, 1] is introduced in BOA, which is implemented by the comparison between a random number in [0, 1] and the parameter P. If the random number is smaller than P, local search phase will be chosen, otherwise global search phase

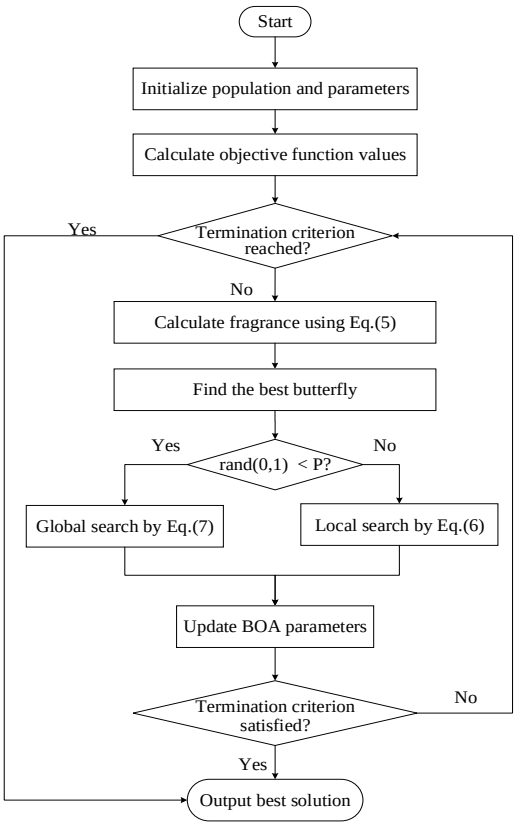

Fig. 1 The flowchart of the BOA

is the alternative. Therefore, the parameter *P* is crucial to control the performance of exploring the search space and exploiting the solutions.

The main process of BOA to identify structural damage is shown in Fig. 1, which mainly includes three phases:

Phase 1: initialize population and predefine various parameters;

Phase 2: employ BOA to minimize objective function until the predefined maximum iteration number reached or the convergence criteria in Eq. (8) satisfied

$$error^{i} = \frac{\left\|\alpha^{i} - \alpha^{i-1}\right\|}{\left\|\alpha^{i-1}\right\|} \times 100\% < Tol \tag{8}$$

where $error^{i}$ stands for the error after *i*-th iteration; α^{i} and α^{i-1} represent the identified structural damage index parameter vector at the *i*-th, and (*i*-1)-th iteration, and *Tol* means the convergence tolerance.

Phase 3: output global optimal solution, including damage location and extent of structure.

3.2 Standard differential evolution algorithm

The differential evolution (DE) is a typical population-based intelligent algorithm by simulating the biological evolution mechanism of nature, mainly including four steps: initialization, mutation, crossover, selection (Mallipeddi *et al.* 2011).

3.2.1 Initialization

In DE, each candidate in the population of *NP* is randomly generated in the search space as

$$\theta_{ij} = \theta_{ij}^{l} + rand(0,1) \times \left(\theta_{ij}^{u} - \theta_{ij}^{l}\right), \quad i = 1,2 \ldots, NP, \quad j = 1,2 \tag{9}$$

where θ_{ij} stands for the *j*-th vectors of candidate θ_i ; θ_{ij}^{u} and θ_{ij}^{l} denote the upper and lower boundary of the search domain; $rand(0,1)$ is a random number uniformly distributed over the interval [0, 1]; *NP* and *N* are the size of population and the number of variable vector, respectively.

3.2.2 Mutation

It is a remarkable feature of DE to realize individual variation through differential strategy, rendering it effective to generate candidate solution. In the mutation step, two different individual vectors are randomly selected from population and subtracted each other to generate a difference vector, then multiplying a weighting coefficient to the difference vector and adding to a third individual vector. The mutation operation is

$$S_i^{G+1} = \theta_{r1}^{G} + F \times (\theta_{r2}^{G} - \theta_{r3}^{G}) \tag{10}$$

where S_i^{G+1} stands for the mutation vector, namely, the new candidate solution; θ_{r1}^{G}, θ_{r2}^{G} and θ_{r3}^{G} denote three different candidate solution at *G*-th generation, randomly chosen from the population of *NP*; *F* is the mutation operator determining the amplification of the difference vector within the range of [0, 2].

3.2.3 Crossover

To increase the diversity of the population, binomial crossover process is applied after mutation operation. The mutated vector S_i^{G+1} intersects with an original individual vector θ_i^{G} to generate a trial vector T_i^{G+1} according to following rules

$$T_{ij}^{G+1} = \begin{cases} S_{ij}^{G+1} \ if \left(rand\left(j\right) \le CR\right) or \left(j = randn\left(i\right)\right) \\ \theta_{ij}^{G} \quad otherwise \end{cases} \tag{11}$$

$$T_{ij}^{G+1} = \begin{cases} S_i^{G+1} \ \text{if} \ (rand(j) \le CR) \ \text{or} \ \left(j = randn(i)\right) \\ \theta_{ij}^{G} \quad \text{otherwise} \end{cases} \tag{11}$$

where $i = 1,2 \ldots, NP$, $j = 1,2, \ldots N$; $rand(j)$ is a random number taken from [0, 1]; $randn(i)$ is an integer randomly chosen from 1 to *NP*; *CR* denotes crossover operator within [0, 1].

3.2.4 Selection

To keep the better candidate solution, greedy selection is performed after evaluation of each candidate. The fitness value of the trial vector T_i^{G+1} is compared with that of original individual vector θ_i^{G} and the better one is retained (Tang *et al*. 2008)

$$\theta_i^{G+1} = \begin{cases} T_i^{G+1} & f(T_i^{G+1}) \le f(\theta_i^{G}) \\ \theta_i^{G} & \text{otherwise} \end{cases} \tag{12}$$

The latter three steps will continue until the termination criterion is met.

3.3 Hybrid butterfly optimization and differential evolution algorithm

In BOA, concentrating on local search is more likely to fall into local optimum, on the contrary, focusing on more global search may lead to slow convergence. Therefore, it is necessary to keep a balance between global exploration and local exploitation in view of accuracy and efficiency of identification results. In this paper, the hybrid algorithm HBODEA, introducing the adaptive mutation and crossover operation of DE into BOA, is proposed to further improve the global search capability of the BOA as well as retain its excellent local search ability.

It is noted that the parameters such as mutation operator and crossover operator have significant effect on performance of algorithm, which are constant in the original DE (Tang *et al*. 2008, Seyedpoor *et al*. 2018a). To find suitable coefficients for mutation and crossover operator, a strategy of trial-and-error search is usually applied before addressing the optimization problem (Mallipeddi *et al*. 2011). In one aspect, it is obvious that the trial-and-error procedure would inevitably consume plenty of computational resources for a good estimation of these two coefficients. In the other aspect, these two estimated constant operator coefficients are quite suitable in the early stage of search, but may have difficulties to achieve a good performance after initial search. Therefore, to improve performance of the proposed HBODEA, a new mutation operation is applied in Eq. (13), owing to its excellent global search capability

$$S_i^{G+1} = \theta_i^G + F \times (\theta_{r1}^G - \theta_{r2}^G + \theta_{r3}^G - \theta_{r4}^G) \times f_i \tag{13}$$

where S_i^{G+1} represents the new mutation vector; r_1, r_2, r_3, r_4 are random integers taken from [1, *NP*] with the constraints $r_1 \neq r_2 \neq r_3 \neq r_4 \neq i$; F is an adaptive mutation operator varied with the iteration number as

$$F = F_0 \times 2^{\gamma}, \qquad \gamma = e^{1-\frac{G_m}{G_m+1-G}} \tag{14}$$

where F_0 is the initial value of the mutation operator, whose value is 0.35 in this study; G_m stands for the maximum number of iterations, and G denotes the current iteration number.

An adaptive crossover operator, varying with the fitness value, is introduced in the proposed HBODEA

$$CR_i = CR_{min} + (CR_{max} - CR_{min}) \times \frac{f_i - f_{min}}{f_{max} - f_{min}} \tag{15}$$

where f_{max} and f_{min} are the best and worst individual fitness values in the current population, respectively; CR_{max} and CR_{min} are the upper and lower boundary, whose values adopted are 0.7 and 0.3, respectively.

In addition, in original BOA, sensor modality C is taken

Step 1. The initialization phase
- Set the size of population *NP*, the dimension of problem *N*, termination criterion, initial value of the mutation operator F_0, crossover operator CR_{max} *and* CR_{min}
- Define sensor modality *C*, power exponent *A* and switch probability *P*
- Generate initial population of butterflies in search domain using Eq. (4)
- Define objective function $f(\mathbf{x})$, calculate stimulus intensity *I*

Step 2. The iteration phase
- **While** termination criterion is not reached **do**
  - **For** butterfly *i* = 1 to *NP* **do**
    - Calculate fragrance using Eq. (5)
  - **End for**
  - Sort fitness values and find the best butterfly g_i^*
  - **For** butterfly *i* = 1 to *NP* **do**
    - Produce a random number uniformly distributed over the interval [0, 1]
    - **If** *rand*(0,1) < *P*
      - Update the butterfly population using Eq. (6)
    - **Else**
      - Update solution by mutation using Eq. (13)
    - **End if**
  - **End for**
  - Update solution by crossover using Eq. (11)
  - Update parameters *F*, *CR*, *C* using Eqs. (14), (15), (16) respectively
  - Greedy selection strategy is used in every iteration to find better solutions
- **End while**

Step 3. Output results
- Output the best solution and optimal value

Fig. 2 The flowchart of HBODEA

as a constant, whereas in the proposed HBODEA the value of the C is varied with the iterations by

$$C^{G+1} = C^{G} \times \left(1 + 0.01 \times \frac{G_m}{G}\right) \tag{16}$$

where G_m stands for the maximum number of iterations and G denotes the current iteration number. It is obvious that the values of the C will increase with the iterations of the algorithm, resulting in generation of diverse candidates to reduce the chance of entrapment in local optima. Fig. 2 presents the whole implementation procedure of the proposed HBODEA.

4. Numerical simulation

Two numerical examples of a simply supported beam and a 37-bar truss structure are employed to verify the effectiveness and robustness of the proposed HBODEA. Meanwhile, BOA and DE are introduced for comparison study. The parameters from paper of Arora and Singh (2018) for BOA and DE are employed in this paper, listed in Table 1. This numerical simulation assumes that the mass parameter is known and stiffness parameter needs to be identified for each element of these two structures.

4.1 A simply supported beam

As shown in Fig. 3, a simply supported beam of 960 mm length, 50 mm width and 3 mm height is modeled with 16 identical beam elements (i.e., n = 16), resulting in element length of 60 mm. Among 17 nodes totally, each node has two degrees of freedom, namely, a vertical translation and a rotation. Due to the large ratio of beam length to its height, Euler-Bernoulli beam theory is applied with ignored shear strain. The Young's modulus and mass density of the simply supported beam are 2.1×10^{11} N/m^2 and 7860 kg/m^3, respectively. There is an ambient excitation which has zero mean and unit standard deviation acting at node 5, as shown in Fig. 3 in vertical direction. The acceleration responses are calculated with Newmark's constant acceleration method, which will be used for structural damage identification. As highlighted in Fig. 3, six accelerometers are installed to obtain dynamic responses in vertical direction with sampling rate of 2000 samples/s and total record time of 2 s.

Table 1 Parameters of three algorithms used for structural damage detection

Parameters	BOA	DE	HBODEA
Population size *NP*	60	60	60
Maximum iteration G_m	200	200	200
Termination criterion *TOL* (tolerance)	10^{-3}	10^{-3}	10^{-3}
Mutation operator *F*		0.5	Eq. (14)
Crossover operator *CR*		0.5	Eq. (15)
Sensor modality *C*	0.01		Eq. (16)
Power exponent *A*	0.1		0.1
Switch probability *P*	0.8		0.8

Some extent of damages is introduced in the 2nd, 4th and 10th elements, modeled by 30%, 20% and 20% reduction of the stiffness, indicating damage index $\alpha_2 = 0.3$, $\alpha_4 = 0.2$, $\alpha_{10} = 0.2$, respectively. In practice, measurements are inevitably contaminated by noise, leading to adverse effect on accuracy of identification results. To investigate the robustness of the proposed method to measurement noise, white Gaussian noise is added to the clean measurements R_{clean} (Trinh and Koh 2012)

$$R_{mea} = R_{clean} + N_l \ N_{noise} RMS(R_{clean}) \tag{17}$$

where N_l is the noise level, N_{noise} is noise vector of Gaussian distribution randomly generated with zero mean and unit standard deviation, and $RMS(R_{clean})$ denotes the root-mean-square of the clean measurement. In the numerical examples presented in this paper, three levels of noise including 0%, 5% and 10% noise are introduced into the acceleration measurements. The presented identification results in Fig. 4 and Table 2 is the summarized average values based on five times of implementing identification procedure by BOA, DE and HBODEA.

By the results presented in Fig. 4(a) and Table 2, BOA and HBODEA provide satisfactory identification results with uncontaminated measurements, while some unneglected identification error is observed at element 9 and 16 with DE. By the results of 5% noise case presented in Fig. 4(b), it can be observed that damage locations are successfully detected, but damage extent isn't accurately identified by BOA and DE, with maximum relative error 23.65% and 35.1%, respectively. On the contrary, HBODEA provides more competitive results with maximum relative error of 6.2%. For 10% noise case, DE has some difficulties to accurately identify damage extent of the 10th element with relative error up to 54.3%. Although BOA acquires more accurate damage index for α_4, obvious

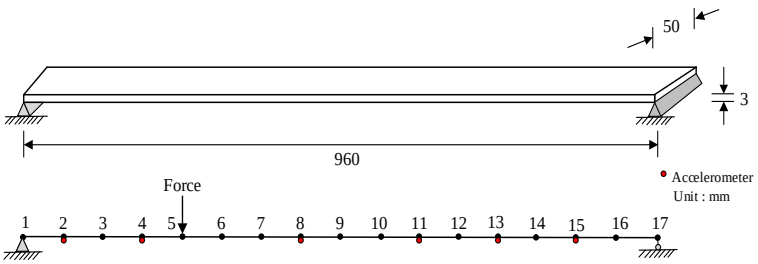

Fig. 3 Numerical model of the simply supported beam

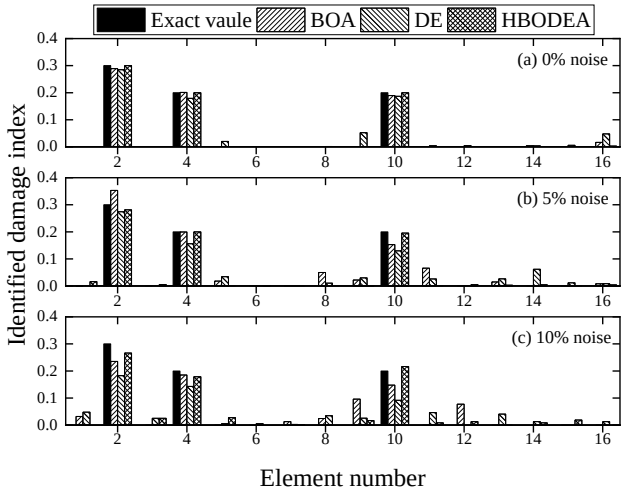

Fig. 4 Identified results with (a) 0% noise; (b) 5% noise; (c) 10% noise

Table 2 Identified damage index for simply supported beam structure (%)

Noise level	Damage extent	BOA		DE		HBODEA	
		Mean	Relative error	Mean	Relative error	Mean	Relative error
0	$\alpha_2 = 20$	28.89	3.70	28.48	5.07	**29.99**	0.03
	$\alpha_4 = 20$	20.11	0.55	17.89	10.55	**20.00**	0.00
	$\alpha_{10} = 20$	18.93	5.35	18.67	6.65	**19.98**	0.10
5	$\alpha_2 = 30$	35.29	17.63	27.41	8.63	**28.14**	6.20
	$\alpha_4 = 20$	19.94	0.30	15.62	21.90	**19.98**	0.10
	$\alpha_{10} = 20$	15.27	23.65	12.98	35.10	**19.56**	2.20
10	$\alpha_2 = 30$	23.54	21.53	18.27	39.10	**26.62**	11.27
	$\alpha_4 = 20$	18.49	7.55	14.29	28.55	**17.87**	10.65
	$\alpha_{10} = 20$	14.79	26.05	9.14	54.3	**21.63**	8.15

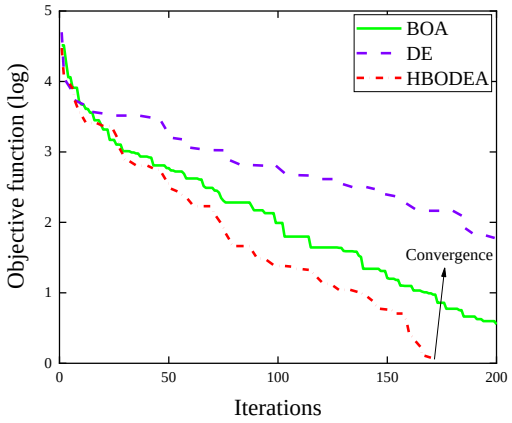

Fig. 5 Convergence process of fitness (noise free)

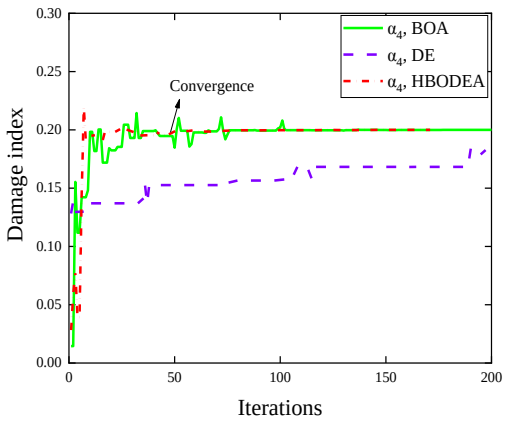

Fig. 6 Convergence process of α_4 (noise free)

false identification occurs at the 9th and 12th elements. The identification results from proposed HBODEA are acceptable with maximum relative error of 11.27% as well as without apparent false identification, which indicate that the proposed HBODEA is more robust to accurately identify structural multiple damages with limited sensors and polluted measurements.

It is showed that more accurate identification results are achieved with the proposed HBODEA compared with those from BOA and DE. In addition, the convergence study results of BOA, DE and HBODEA are shown in Fig. 5, and it is observed that HBODEA provides the identification results owing to the satisfied convergence criterion before the maximum iteration number reached, and BOA and DE

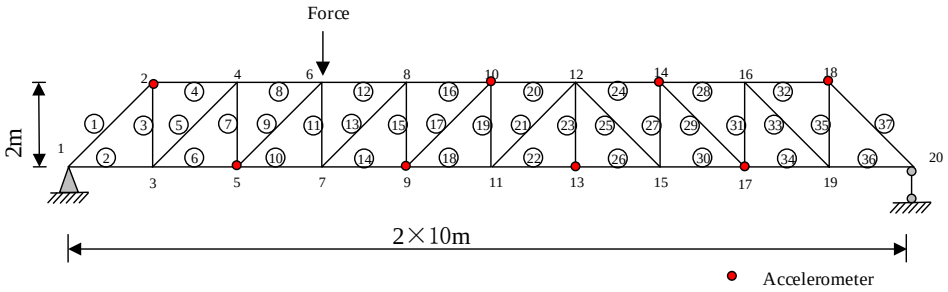

Fig. 7 Numerical model of the plane 37-bar truss structure

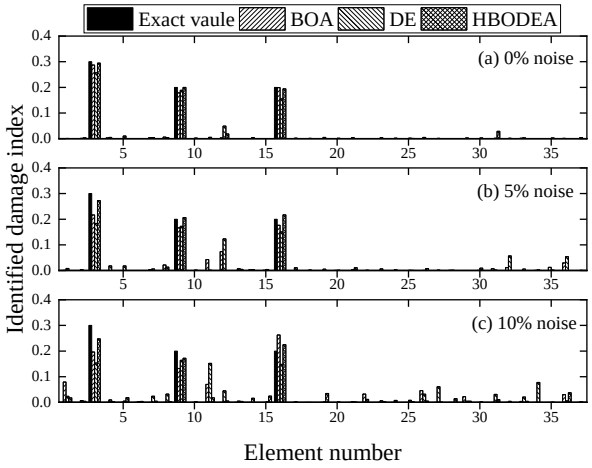

Fig. 8 Identified results with (a) 0% noise; (b) 5% noise; (c) 10% noise

still has significant discrepancy between the estimated and measured structural acceleration responses with maximum iteration reached, indicating excellent performance of HBODEA in terms of accuracy and efficiency.

In addition, the convergence processes of element damage index α_4 is taken for example to compare the performance of the three algorithms, shown in Fig. 6. It is found that only around 50 iterations are needed for HBODEA to converge to the exact value, while around 100 iterations are required for BOA still accompanied with fluctuations afterwards, and DE needs more than 200 iterations to achieve convergence.

4.2 A 37-bar truss structure

As shown in Fig. 7, to examine the performance of HBODEA, the second numerical study is carried on a plane 37-bar truss structure, consisting of 37 elements connected by 20 nodes. The boundary condition of truss is modeled as a pin support at node 1 and a roller support at node 20. The cross-sectional area of each element is 0.0016 m^2 and the Young's modulus and mass density are 2.1×10^{11} N/m^2 and 7.8×10^3 kg/m^3, respectively. An ambient excitation with magnitude of 200 N, zero mean and unit standard deviation is applied at node 6 in vertical direction, and eight accelerometers shown in Fig. 7 are employed to obtain dynamic responses in vertical direction for 2 s with sampling rate of 2000 samples/s. It is assumed that there are 30%, 20%, 20% reduction of the stiffness at the 3th, 9th, 16th elements, implying damage index α_3=0.3, α_9=0.2, α_{16}=0.2, respectively. The effect of measurement noise on the performance of the proposed method is investigated by introduction of 0%, 5% and 10% white Gaussian noise. After five times of computation with BOA, DE and HBODEA, the summarized average identification results are displayed in Fig. 8 and Table 3.

It is noted that the proposed three algorithms are able to accurately detect the damage locations with uncontaminated measurements, and the identified damage index in Table 3 shows that the hybrid algorithm supplies more accurate identification results, with maximum relative error only 2.8%. By the results of 5% noise case, HBODEA provides

Table 3 Identified damage index for the 37-bar truss structure (%)

Noise level	Damage extent	BOA		DE		HBODEA	
		Mean	Relative error	Mean	Relative error	Mean	Relative error
0	α_3 = 30	28.71	4.30	25.68	14.40	**29.47**	1.77
	α_9 = 20	17.89	10.55	18.88	5.60	**19.98**	0.10
	α_{16} = 20	19.88	0.60	15.54	22.30	**19.44**	2.80
5	α_3 = 30	21.65	27.83	18.34	38.87	**27.28**	9.07
	α_9 = 20	16.57	17.15	17.24	13.80	**20.67**	3.35
	α_{16} = 20	17.65	11.75	15.05	24.75	**21.69**	8.45
10	α_3 = 30	19.61	34.63	15.33	48.90	**24.75**	17.5
	α_9 = 20	13.23	33.85	16.39	18.05	**17.19**	14.05
	α_{16} = 20	26.26	31.30	14.82	25.90	**22.48**	12.40

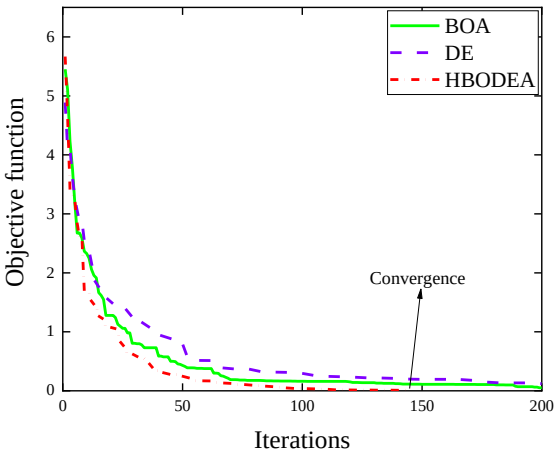

Fig. 9 Evolutionary process of fitness (noise free)

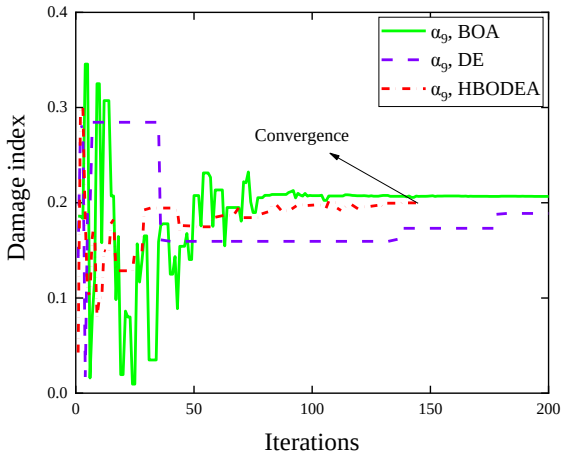

Fig. 10 Convergence process of α_9 (noise free)

more accurate identification results with the maximum relative error 9.07%, compared with 27.83% and 38.87% from BOA and DE. When noise level increases to 10%, the maximum relative errors of BOA, DE and HBODEA increase to 34.63%, 48.9%, and 17.5%, but the proposed hybrid algorithm still presents a better performance. By the identification results in Fig. 8 and Table 3, it is concluded that increase of noise level leads to a significant increase in the identification error, implying its significant impact on the accuracy of identification results, however, the proposed HBODEA exhibit better performance compared with BOA and DE.

Furthermore, the convergence study of BOA, DE, and HBODEA is also conducted, shown in Fig. 9 and the iteration process of the identified damage index α_9 is presented in Fig. 10. It is observed that HBODEA takes less than 150 iterations to meet the convergence criteria but DE and BOA obtain the solution due to the maximum iteration number reached, implying fast convergence rate of HBODEA.

5. Experimental verification

Laboratory studies on an 8-story shear-type steel frame is conducted to validate the proposed structural damage identification method with experimental testing data.

5.1 Experimental setup and initial model updating

The tested steel frame with height of 2 m and width of 0.6 m is shown in Fig. 11. The frame consists of eight identical steel floors and two steel columns with same size, as shown in Fig. 11(b). The geometries for steel floors are 600×100×25 mm and steel columns have the dimension of 2000×50×5 mm. The steel floors and columns of frame are welded together, and the frame is a typical shear-type structure due to strong floors and comparatively weak column with the cross-section ratio of 10. The bottom end of frame is welded to a large and thick steel plate. The mass density and elastic modulus of the steel frame are 7850 kg/m^3 and 2.0×10^{11} N/m^2.

To get dynamic characteristics of steel frame structure, its free vibration data in horizontal direction is recorded by the installed accelerometers at each floor at sampling rate of

(a) Model

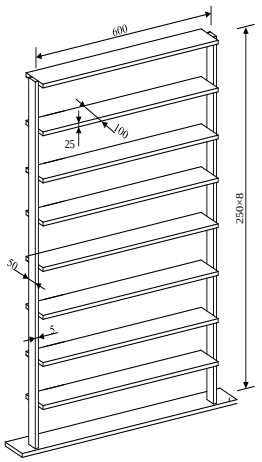

(b) Dimensions

(c) Finite element model

Fig. 11 The laboratory tested steel frame

Table 4 Measured and calculated natural frequencies before and after updating

Mode	Measured	Before updating		After updating	
	(HZ)	Analytical (Hz)	Relative error (%)	Analytical (Hz)	Relative error (%)
1	4.645	4.718	1.577	**4.645**	0.002
2	13.705	13.793	0.648	**13.704**	0.007
3	22.554	22.959	1.798	**22.558**	0.018
4	30.695	30.902	0.676	**30.701**	0.019
5	38.241	38.293	0.138	**38.247**	0.016
6	44.434	44.252	0.411	**44.444**	0.023
7	48.826	48.332	1.012	**48.791**	0.072
8	52.306	51.464	1.609	**52.421**	0.220

1024 samples/s after a hit by a hammer with rubber tip. The measured natural frequencies are extracted from the measured accelerations with aid of Fast Fourier Transfer technique, listed in Table 4. As shown in Fig. 11(c), the frame is simplified as a lumped-mass finite element model, which would inevitably introduce the modelling error during the process of structural parameter identification. To alleviate the adverse effect of modeling error on the accuracy of identification results, an initial model updating is implemented by updating elemental stiffness parameters of the analytical model with vibration testing data.

Vibration test was performed by using the hammer to hit at every floor of the tested steel frame, and total eight acceleration responses are recorded for 60 s for computation of measured natural frequencies. The stiffness and natural frequencies are updated by the proposed HBODEA with objective function of minimizing the discrepancy between the measured and the calculated natural frequencies. The stiffness and natural frequencies of before and after model updating are shown in Fig. 12 and Table 4, and the lumped-mass finite element model is validated by the small discrepancy between the measured and analytical natural frequencies before updating. To minimizing the influence of modeling error, the updated stiffness values are taken as the baseline for the next damage detection.

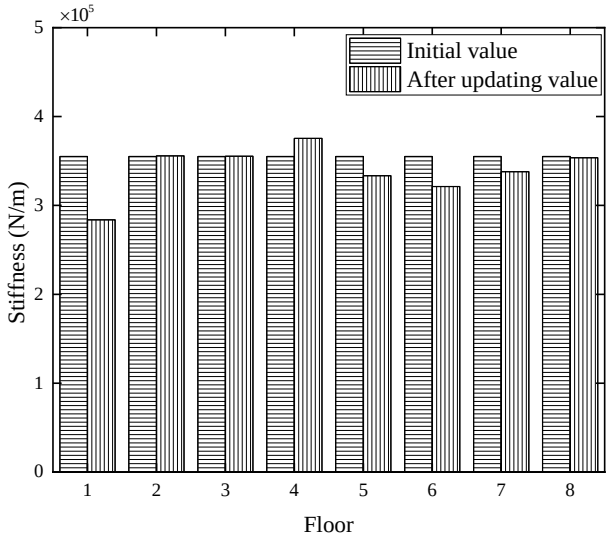

Fig. 12 Stiffness of before and after model updating

5.2 Damage identification for the tested structure

In this experiment, damage is introduced by cutting the columns of tested steel frame. As shown in Fig. 13, 40% cross section is reduced in one column at the 2th floor of the frame, indicating 20% reduction of the equivalent stiffness, namely $\alpha_2 = 0.2$. In fact, cutting the cross section of columns would inevitably lead to reduction of mass and stiffness of the frame, which are suggested to be identified simultaneously from a practice point of view. Nevertheless, mass remains unchanged since only around 3% slight reduction of mass caused by this damage in the lumped-mass model, and such small variation of mass is difficult to be accurately identified. With the same parameter settings of the numerical simulation in Table 1, BOA, DE and HBODEA are employed to detect damage of the frame, and the identification results are shown in Fig. 14.

The results in Fig. 14 show that three methods in this paper give reliable identified damage location and extent with vibration data. The identified relative errors of the 2th floor by BOA, DE and HBODEA are 16.31%, 17.09% and 3.4%, which illustrates excellent performance of the proposed HBODEA. In addition, the observed maximum false identification 5.23%, 5.45% and 2.17% by BOA, DE and HBODEA further demonstrates that the proposed HBODEA can accurately identify structural damage even

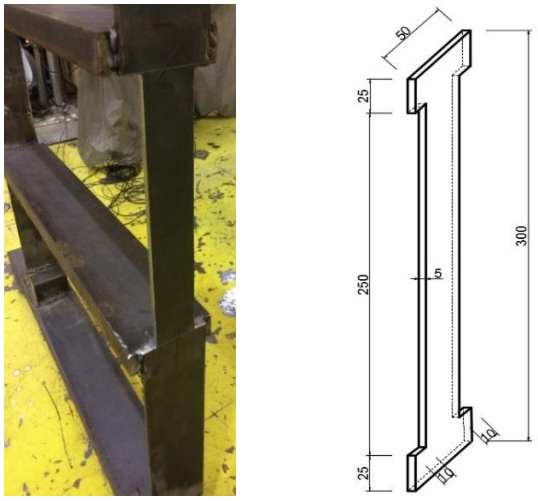

Fig. 13 20% reduction of stiffness in the second floor

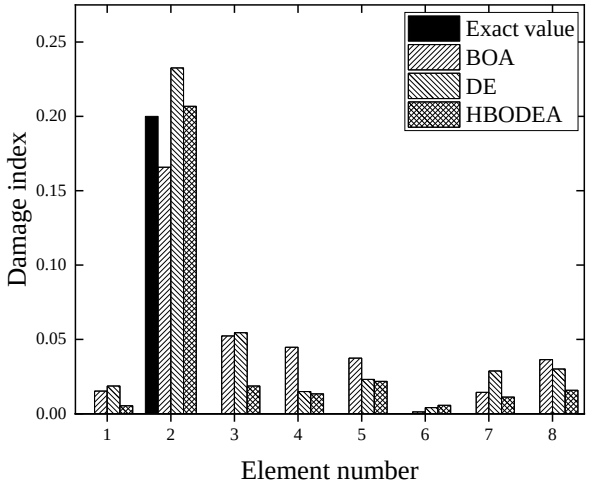

Fig. 14 Identified results of steel frame

with modelling error by assumed constant mass and environmental noise.

6. Discussion

6.1 Search space

To examine the robustness of search space range on the accuracy of identification results with BOA, DE and HBODEA, the numerical study on a simple 13-bar truss model shown in Fig. 15 is carried out. The 13-bar truss structure has same cross-sectional area and material properties with 37-bar truss structure. There is an ambient excitation with zero mean and unit standard deviation applied at node 4 in vertical direction, and its magnitude is 200 N. In addition, three accelerometers highlighted in Fig. 15 are installed to measure dynamic responses with same sampling rate of the 37-bar truss structure.

For convenience, define $\delta_i = 1 - \alpha_i \quad (0 \le \delta_i \le 1)$ as a fraction of the intact stiffness of the *i*-th element, and $\delta_i = 0$ denotes that the *i*-th structural element completely loses its stiffness while $\delta_i = 1$ indicates that the structural element is intact. In this example, three different search spaces of each parameter, namely [0.75, 1.25], [0.5, 1.5] and [0.5, 2.0] of their corresponding exact value are assumed in BOA, DE and HBODEA for comparison study in terms of accuracy and efficiency of identification results.

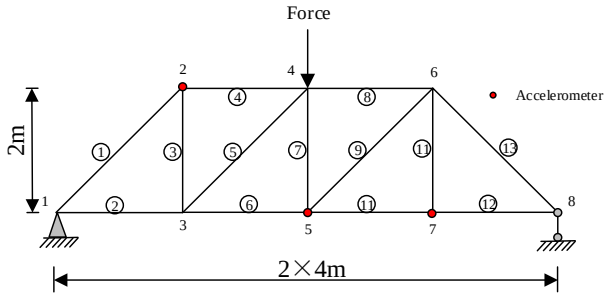

Fig. 15 Numerical model of the plane 13-bar truss structure

The corresponding identification results are shown in Fig. 16 and identification error is presented in Table 5.

By the results presented in Fig. 16 and Table 5, it is clear that identification error increases with search space since the initial value has a significant deviation from the exact value, leading to negative effect on the convergence to the exact value. When search space of δ is [0.75, 1.25] times of their corresponding exact values, excellent identification results are achieved with BOA, DE and HBODEA with maximum error of 1.42%, 1.67% and 0.36%, respectively. When the search range increases to [0.5, 1.5] of the exact values, the identification maximum error increases to 6.84%, 2.51% and 1.84% for BOA, DE and HBODEA, respectively. It is shown that BOA provides unfavorable results compared with DE and HBODEA. When the search range continues to increase to [0.5, 2.0] of the exact values, there is a significant increase in the maximum identification error, namely 18.79%, 6.39% and 3.11% for BOA, DE and HBODEA, respectively. It is concluded that BOA is more sensitive to the search space range, implying heavy dependence on the initial guess of unknown parameters. Due to the relatively weak exploration capability, it would possibly provide unsatisfactory identification results or even fall into local optima with wide search space or imperfect

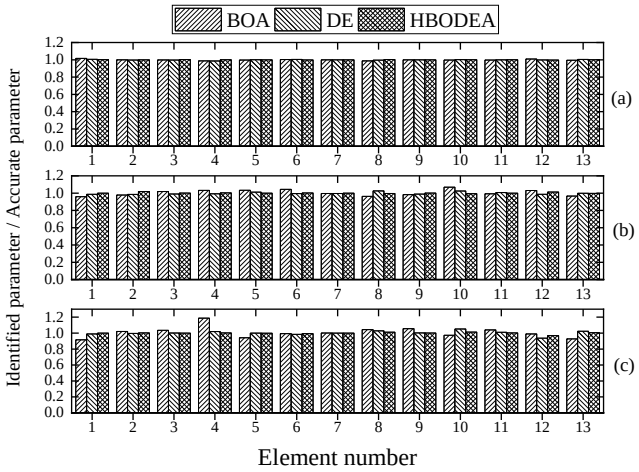

Fig. 16 Identification results with search spaces
(a) [0.75, 1.25]; (b) [0.5, 1.5]; (c) [0.5, 2.0]

Table 5 Identification error with different search space (%)

Search spaces	BOA		DE		HBODEA	
	Max error	Mean error	Max error	Mean error	Max error	Mean error
[0.75, 1.25]	1.42	0.54	1.67	0.33	**0.36**	**0.13**
[0.5, 1.5]	6.84	2.99	2.51	1.14	**1.84**	**0.41**
[0.5, 2.0]	18.79	4.95	6.39	1.76	**3.11**	**0.61**

parameters setup of BOA, such as sensor modality C, power exponent A, switch probability P, etc. In general, owing to its powerful global search ability, DE has a pleasant performance with acceptable identification results due to the embedded mutation and crossover operations for broad search. Among these three methods, the hybrid method presents the best results, implying that introduction of the mutation and crossover operators of DE into BOA is beneficial to improve its global search ability without compromising its local search capacity.

To further evaluate the performance of these three methods in aspect of computational efficiency, the convergence process and computational time for these three methods are shown in Fig. 17 and Table 6. With search space [0.75, 1.25] of the exact values for each parameter, BOA and DE needs 190 and 200 iteration to achieve the converged identification results, but HBODEA only takes 150 iterations to satisfy the convergence criteria, resulting in less computation resources consumption for the proposed hybrid strategy with similar consumed time for each iteration. With wide search space [0.5, 1.5] and [0.5, 2.0] of the exact values applied for each parameter, BOA, DE and HBODEA provide their converged results with maximum iteration number reached. Although similar computational resources are exhausted for these three methods, the proposed HBODEA provides more favorable identification with negligible identification error, demonstrating its merit of high computational efficiency compared with BOA and DE. Therefore, in the proposed hybrid algorithm, effective combination of the strong exploitation capability of BOA and exploration capability of DE can balance the computation resources on global and search to detect structural damages accurately and efficiently.

6.2 Dynamic operator

In the proposed HBODEA, dynamic mutation and crossover operators shown in Eqs. (14)-(15) are introduced to further improve its performance. Therefore, to investigate truss structure is still employed, and search space is defined as [0.5, 2.0] of their corresponding exact values. The final identified error is presented in Fig. 18, which shows that the dynamic operators contribute to produce more accurate identification results compared with those of applied constant operators.

Table 7 Operator setups of DE and HBODEA

Operator	DE1	DE2	DE3	HBODEA
F	0.5	0.5	0.7	Eq. (14)
CR	0.5	0.8	0.3	Eq. (15)

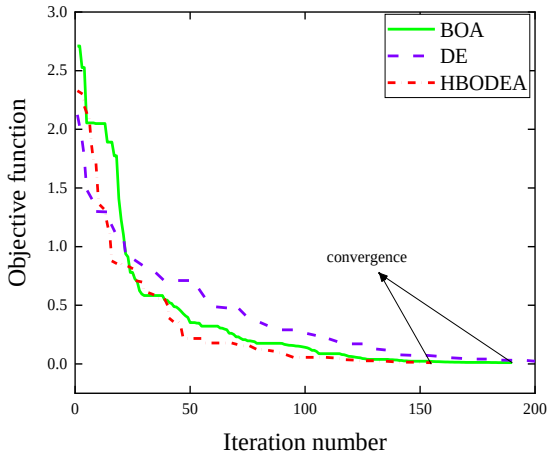

Fig. 17 The convergence process with [0.75, 1.25] search space

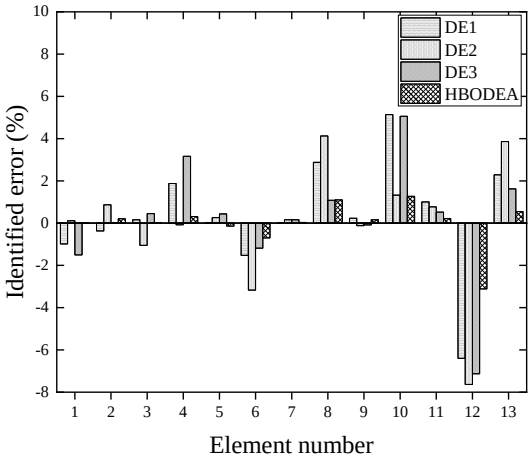

Fig. 18 Identified error with DE and HBODEA

Table 6 Computational time for the proposed three methods in three search spaces

Search space	Methods	Number of iterations	Time for single iteration (s)	Total time (s)
[0.75, 1.25]	BOA	190	10.85	2062
	DE	200	11.23	2246
	HBODEA	155	10.91	1693
[0.5, 1.5]	BOA	200	10.82	2164
	DE	200	11.19	2238
	HBODEA	200	10.87	2175
[0.5, 2.0]	BOA	200	10.80	2160
	DE	200	11.07	2214
	HBODEA	200	10.85	2166

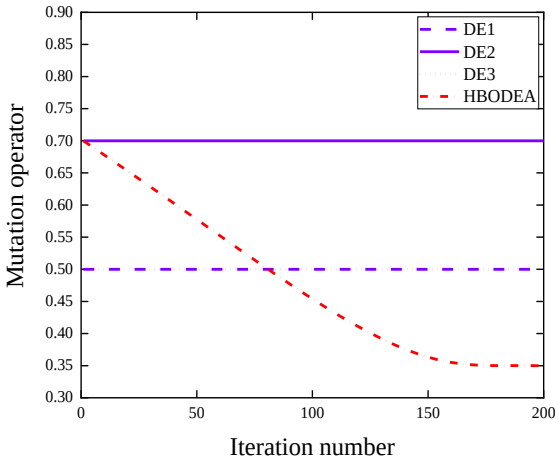

Fig. 19 Mutation operator over the process of the iterations

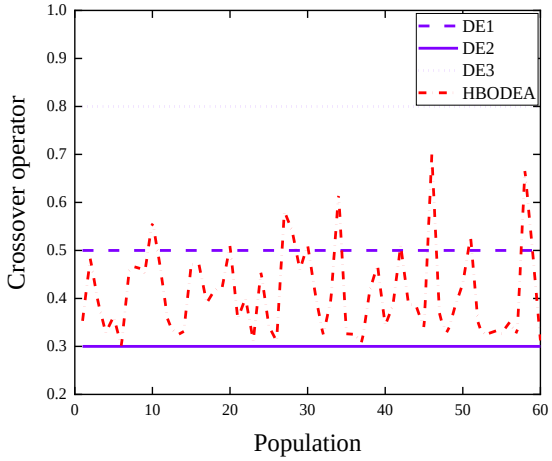

Fig. 20 Value of crossover operator for a population

To further understand the positive effect of the dynamic operators, values of mutation operator in each iteration are demonstrated in Fig. 19. The results show that the dynamic mutation operator offers large mutation rate at initial search stage, which helps to maintain the individual diversity to avoid premature convergence, and the mutation rate gradually decreases with increasing iteration number, which contributes to keep good solution and converge to global optimum. For the constant mutation operator, it may have high possibility to be trapped in local optimum with small mutation rate, and it may suffer slow convergence rate with large mutation rate. It can be concluded that the mutation operator is the most important factor to balance the computational resources between global and local search, and the embedded dynamic mutation operator is capable of reasonably and efficiently assigning the computational resources, since it focuses on global search with large value of mutation rate at early search stage and concentrates on local search with small value when the search is close to the global optimum.

In addition, values of crossover operation for a population are presented in Fig. 20, which show that dynamic crossover operator give each candidate a different crossover rate, mainly determined by its fitness value. For the individuals with high fitness values, small value of crossover rate is applied, resulting in large chance to be

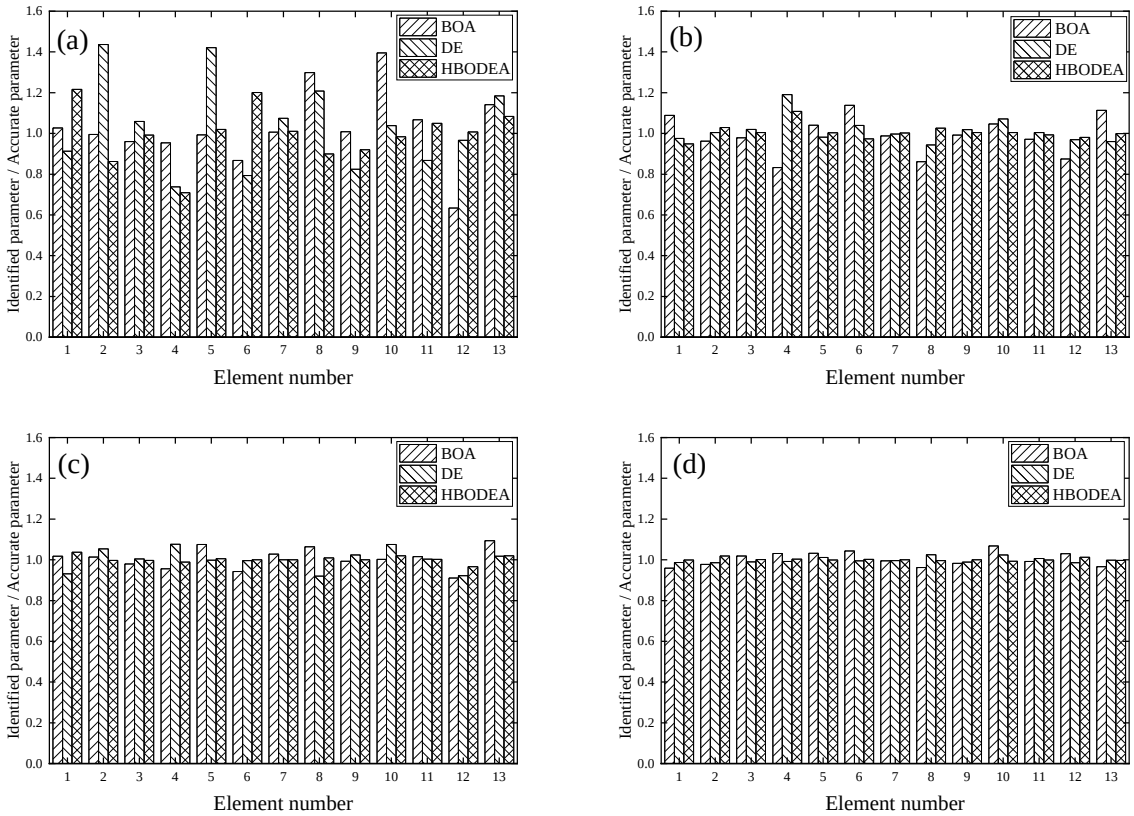

Fig. 21 Identification results with population size (a) 10; (b) 20; (c) 40; and (d) 60

Table 8 Mean and maximum identification error with different population size (%)

Population size	BOA		DE		HBODEA	
	Max error	Mean error	Max error	Mean error	Max error	Mean error
10	39.52	11.87	43.65	17.84	**29.07**	**9.38**
20	16.57	7.44	19.06	4.01	**10.85**	**2.19**
40	9.41	4.08	7.97	3.74	**3.67**	**1.11**
60	6.84	2.99	2.51	1.14	**1.84**	**0.41**

restored in the next population. In contrast, large value is applied to the worst candidates, implying low possibility to survive during generation of the new population. Compared with constant crossover rate, the dynamic value is beneficial to reserve the best individual and eliminate the worst candidates, contributing to improve accuracy and efficiency of the identification results.

6.3 Population size

In general, population size is another important parameter in determining the performance of most swarm intelligence heuristic search methods, since small population size is beneficial for convergence but has high chance to fall into local optimum and large population size can improve search ability but suffers by the slow convergence rate. To investigate the population size on the robustness of the proposed identification strategy, 10, 20, 40 and 60 are considered in the numerical example of the 13-bar truss structure, and search space is defined as [0.5, 1.5]. The final identified results are presented in Fig. 21 and Table 8.

With population size of 10, multiple false identifications are detected, thus none of the three methods can accurately identify structural parameters with very small population size. When the population size increases to 20, although large identification errors are still observed for these three methods, HBODEA provides comparatively better identification results with maximum error of 10.85% and mean error of 2.19%, compared with those of BOA and DE. With large population size of 40 and 60, all these three methods are able to provide satisfactory identification results, but HBODEA performs best in terms of identification accuracy. All these results show that the population size has a significant effect on the accuracy of identification results for these three methods, and improper value of population size would probably lead to converge to local optimum or slow convergence rate. Despite high sensitivity on the population size, HBODEA provides the best identification result with same population size compared with other two methods.

7. Conclusions

In this paper, a hybrid identification strategy, effective incorporation of powerful local exploitation ability of BOA and excellent global exploration capacity of DE, is proposed to detect the presence, location and magnitude of damage in structures. In the proposed strategy, mutation and crossover operations of DE, as well as dynamic adaptive operators are introduced into original BOA to enhance the global search ability without compromising its local search capacity. The performance of proposed hybrid method is examined by two numerical examples, namely a simply supported beam and a 37-bar truss structure, and an experimental study on an 8-story shear-type steel frame. In addition, the effect of search space, two dynamic operators, population size on identification accuracy and efficiency are further investigated. Some conclusions can be summarized:

- The numerical and experimental results show that the proposed HBODEA provides more favorable identification results in terms of accuracy and efficiency compared with BOA and DE. The introduction of dynamic mutation and crossover operations into original BOA is an effective approach to enhance its global search ability, leading to reasonable and efficient assignment of computation resources on global and local search.
- For these three methods, it is found that it has a great possibility to achieve unpleasant identification results with assigned wide search range or small population size, implying their significant influence on the accuracy of identification results. Despite heavy dependence on size of search range or population, HBODEA still has better performance with relatively small maximum and mean identification errors compared with other two methods.
- The two dynamic operators generate adaptive mutation rate in each iteration and crossover rate for each candidate to further improve performance of the proposed strategy. The dynamic mutation operator offers large value of mutation rate during the initial search stage, implying more attention focused on the global exploration, and gradually decreased value of mutation rate, suggesting more engagement of local search with the progressing of seeking the global optimum. In addition, for each candidate, the dynamic crossover operator provides different crossover rate decided by its fitness, which is beneficial to keep the best candidates and eliminate the worst ones.

By the preliminary results presented in this paper, it is found that search space and population size play an important role in the proposed strategy, ongoing research includes appropriate estimation of search space with aid of sampling methods with purpose of identifying parameters with unknown exact values or extremely wide search range, adaptive population size during each iteration to further improve the computation efficiency of proposed strategy.

Declaration of competing interest

The authors declare no conflict of interest.

Acknowledgments

The work was supported by the research project of Beijing Municipal Committee of Education Project KM201810005019, Beijing Natural Science Foundation grant number 8184063, National Natural Science Foundation of China (NSFC) grant number 11872190, 51808017 and 51778028. These financial supports are sincerely appreciated. Besides, the author would like to thank the anonymous reviewers for their detailed and fruitful remarks.

References

Arora, S. and Anand, P. (2018), "Learning automata-based butterfly optimization algorithm for engineering design problems", *Int. J. Comput. Mater. Sci. Eng.*, **7**(4), 1850021. https://doi.org/10.1142/S2047684118500215

Arora, S. and Singh, S. (2015), "Butterfly algorithm with Lèvy Flights for global optimization", *Proceedings of 2015 International Conference on Signal Processing, Computing and Control* (*ISPCC*), Waknaghat, India, September.

Arora, S. and Singh, S. (2017a), "An Effective Hybrid Butterfly Optimization Algorithm with Artificial Bee Colony for Numerical Optimization", *Int. J. Interact. Multimed. Artif. Intell.*, **4**(4). https://doi.org/10.9781/ijimai.2017.442

Arora, S. and Singh, S. (2017b), "Node Localization in Wireless Sensor Networks Using Butterfly Optimization Algorithm", *Arab. J. Sci. Eng.*, **42**(8), 3325-3335. https://doi.org/10.1007/s13369-017-2471-9

Arora, S. and Singh, S. (2018), "Butterfly optimization algorithm: a novel approach for global optimization", *Soft Comput.*, **23**(3), 715-734. https://doi.org/10.1007/s00500-018-3102-4

Blair, R.B. and Launer, A.E. (1997), "Butterfly diversity and human land use: Species assemblages along an urban grandient", *Biol. Conserv.*, **80**(1), 113-125. https://doi.org/10.1016/S0006-3207(96)00056-0

Cao, M.S., Radzienski, M., Xu, W. and Ostachowicz, W. (2014), "Identification of multiple damage in beams based on robust curvature mode shapes", *Mech. Syst. Signal. Pr.*, **46**(2), 468-480. https://doi.org/10.1016/j.ymssp.2014.01.004

Chatzi, E.N. and Fuggini, C. (2015), "Online correction of drift in structural identification using artificial white noise observations and an unscented Kalman filter", *Smart Struct. Syst., Int. J.*, **16**(2), 295-328. https://doi.org/10.12989/sss.2015.16.2.295

Chen, C. and Yu, L. (2019), "A hybrid ant lion optimizer with improved Nelder–Mead algorithm for structural damage detection by improving weighted trace lasso regularization", *Adv. Struct. Eng.*, 1-17. https://doi.org/10.1177/1369433219872434

Dewangan, P., Parey, A., Hammami, A., Chaari, F. and Haddar, M. (2020), "Damage detection in wind turbine gearbox using modal strain energy", *Eng. Fail. Anal.*, **107**, 104228. https://doi.org/10.1016/j.engfailanal.2019.104228

Ding, Z.H., Huang, M. and Lu, Z.R. (2016), "Structural damage detection using artificial bee colony algorithm with hybrid search strategy", Swarm Evol. Comput., 28, 1-13. https://doi.org/10.1016/j.swevo.2015.10.010

Ding, Z.H, Li, J., Hao, H. and Lu, Z.R. (2019), "Structural damage identification with uncertain modelling error and measurement noise by clustering based tree seeds algorithm", *Eng. Struct.*, **185**, 301-314. https://doi.org/10.1016/j.engstruct.2019.01.118

Ding, Z.H., Li, J. and Hao, H. (2020), "Structural damage identification by sparse deep belief network using uncertain and limited data", *Struct. Control. Hlth.*, **27**(5). https://doi.org/10.1002/stc.2522

Doebling, S.W., Farrar, C.R. and Prime, M.B. (1998), "A summary review of vibration-based damage identification methods", *Shock Vib. Dig.*, **30**(2), 91-105. https://doi.org/10.1177/058310249803000201

He, J. and Zhou, Y. (2019), "A novel mode shape reconstruction method for damage diagnosis of cracked beam", *Mech. Syst. Signal. Pr.*, **122**, 433-447. https://doi.org/10.1016/j.ymssp.2018.12.045

Huang, M., Cheng, S., Zhang, H., Gul, M. and Lu, H. (2019), "Structural Damage Identification Under Temperature Variations Based on PSO–CS Hybrid Algorithm", *Int. J. Struct. Stab. Dyn.*, **19**(11), 1950139. https://doi.org/10.1142/S0219455419501396

Huo, L.S., Li, X., Yang, Y.B. and Li, H.N. (2016), "Damage Detection of Structures for Ambient Loading Based on Cross Correlation Function Amplitude and SVM", *Shock Vib.*, 1-12. https://doi.org/10.1155/2016/3989743

Kang, F., Li, J.J. and Xu, Q. (2012), "Damage detection based on improved particle swarm optimization using vibration data", *Soft. Comput.*, **12**(8), 2329-2335. https://doi.org/10.1016/j.asoc.2012.03.050

Kaveh, A., Vaez, S.R.H., Hosseini, P. and Fallah, N. (2016), "Detection of damage in truss structures using Simplified Dolphin Echolocation algorithm based on modal data", *Smart Struct. Syst., Int. J.*, **18**(5), 983-1004. https://doi.org/10.12989/sss.2016.18.5.983

Kim, J.T., Park, J.H., Yoon, H.S. and Yi, J.H. (2007), "Vibration-based damage detection in beams using genetic algorithm", *Smart Struct. Syst., Int. J.*, **3**(3), 263-280. https://doi.org/10.12989/sss.2007.3.3.263

Lee, K.J. and Yun, C.B. (2008), "Parameter identification for nonlinear behavior of RC bridge piers using sequential modified extended Kalman filter", *Smart Struct. Syst., Int. J.*, **4**(3), 319-342. https://doi.org/10.12989/sss.2008.4.3.319

Li, G.C., Shuang, F., Zhao, P. and Le, C.Y. (2019), "An Improved Butterfly Optimization Algorithm for Engineering Design Problems Using the Cross-Entropy Method", *Symmetry-Basel*, **11**(8), 1049. https://doi.org/10.3390/sym11081049

Liang, Y., Feng, Q., Li, H. and Jiang, J. (2019), "Damage detection of shear buildings using frequency-change-ratio and model updating algorithm", *Smart Struct. Syst., Int. J.*, **23**(2), 107-122. https://doi.org/10.12989/sss.2019.23.2.107

Liu, K., Yan, R.J. and Soares, C.G. (2018), "Damage identification in offshore jacket structures based on modal flexibility", *Ocean Eng.*, **170**, 171-185. https://doi.org/10.1016/j.oceaneng.2018.10.014

Lu, Y. and Gao, F. (2005), "A novel time-domain auto-regressive model for structural damage diagnosis", *J. Sound. Vib.*, **283**(3-5), 1031-1049. https://doi.org/10.1016/j.jsv.2004.06.030

Lu, Z.R. and Wang, L. (2017), "An enhanced response sensitivity approach for structural damage identification: convergence and performance", *Int. J. Numer. Methods Eng.*, **111**(13), 1231-1251. https://doi.org/10.1002/nme.5502

Maity, D. and Tripathy, R.R. (2005), "Damage assessment of structures from changes in natural frequencies using genetic algorithm", *Struct. Eng. Mech., Int. J.*, **19**(1), 21-42. https://doi.org/10.12989/sem.2005.19.1.021

Mallipeddi, R., Suganthan, P.N., Pan, Q.-K. and Tasgetiren, M.F. (2011), "Differential evolution algorithm with ensemble of parameters and mutation strategies", *Appl. Soft. Comput.*, **11**(2), 1679-1696. https://doi.org/10.1016/j.asoc.2010.04.024

Mirzaee, A., Shayanfar, M. and Abbasnia, R. (2015), "A novel sensitivity method to structural damage estimation in bridges with moving mass", *Struct. Eng. Mech., Int. J.*, **54**(6), 1217-1244. https://doi.org/10.12989/sem.2015.54.6.1217

Padil, K.H., Bakhary, N., Abdulkareem, M., Li, J. and Hao, H.

(2020), "Non-probabilistic method to consider uncertainties infrequency response function for vibration-based damage detection using Artificial Neural Network", *J. Sound. Vib.*, **467**. https://doi.org/10.1016/j.jsv.2019.115069

Pan, C.D., Yu, L., Chen, Z.P., Luo, W.F. and Liu, H.L. (2016), "A hybrid self-adaptive Firefly-Nelder-Mead algorithm for structural damage detection", *Smart Struct. Syst., Int. J.*, **17**(6), 957-980. https://doi.org/10.12989/sss.2016.17.6.957

Raguso, R.A. (2008), "Wake up and smell the roses: the ecology and evolution of floral scent", *Annu. Rev. Ecol. Evol. Syst.*, **39**, 549-569. https://doi.org/10.1146/annurev.ecolsys.38.091206.095601

Seyedpoor, S.M., Ahmadi, A. and Pahnabi, N. (2018a), "Structural damage detection using time domain responses and an optimization method", *Inverse Probl. Sci. Eng.*, **27**(5), 669-688. https://doi.org/10.1080/17415977.2018.1505884

Seyedpoor, S.M., Norouzi, E. and Ghasemi, S. (2018b), "Structural damage detection using a multi-stage improved differential evolution algorithm (Numerical and experimental)", *Smart Struct. Syst., Int. J.*, **21**(2), 235-248. https://doi.org/10.12989/sss.2018.21.2.235

Singh, B. and Anand, P. (2019), "A novel adaptive butterfly optimization algorithm", *Int. J. Comput. Mater. Sci. Eng.*, **7**(4), 1850026. https://doi.org/10.1142/s2047684118500264

Sotoudehnia, E., Shahabian, F. and Sani, A.A. (2019), "An iterative method for damage identification of skeletal structures utilizing biconjugate gradient method and reduction of search space", *Smart Struct. Syst., Int. J.*, **23**(1), 45-60. https://doi.org/10.12989/sss.2019.23.1.045

Stutz, L., Tenenbaum, R. and Correa, R. (2015), "The Differential Evolution method applied to continuum damage identification via flexibility matrix", *J. Sound Vib.*, **345**, 86-102. https://doi.org/10.1016/j.jsv.2015.01.049

Tang, H., Xue, S. and Fan, C. (2008), "Differential evolution strategy for structural system identification", *Comput. Struct.*, **86**(21-22), 2004-2012. https://doi.org/10.1016/j.compstruc.2008.05.001

Trinh, T.N. and Koh, C.G. (2012), "An improved substructural identification strategy for large structural systems", *Struct. Control. Hlth.*, **19**(8), 686-700. https://doi.org/10.1002/stc.463

Vo-Duy, T., Ho-Huu, V., Dang-Trung, H. and Nguyen-Thoi, T. (2016), "A two-step approach for damage detection in laminated composite structures using modal strain energy method and an improved differential evolution algorithm", *Compos. Struct.*, **147**, 42-53. https://doi.org/10.1016/j.compstruct.2016.03.027

Vosoughi, A.R. (2015), "A developed hybrid method for crack identification of beams", *Smart Struct. Syst., Int. J.*, **16**(3), 401-414. https://doi.org/10.12989/sss.2015.16.3.401

Wang, X.J., Zhang, G.C., Wang, X.M. and Ni, P.H. (2020), "Output-only structural parameter identification with evolutionary algorithms and correlation functions", *Smart Mater. Struct.*, **29**(3). https://doi.org/10.1088/1361-665X/ab6ce9

Wickramasinghe, W.R., Thambiratnam, D.P. and Chan, T.H.T. (2020), "Damage detection in a suspension bridge using modal flexibility method", *Eng. Fail. Anal.*, **107**, 104194. https://doi.org/10.1016/j.engfailanal.2019.104194

Yang, J.N., Huang, H.W. and Pan, S.W. (2009), "Adaptive Quadratic Sum-Squares Error for Structural Damage Identification", *J. Eng. Mech-Asce.*, **135**(2), 67-77. https://doi.org/10.1061/(ASCE)0733-9399(2009)135:2(67)

Yi, T.H., Li, H.N. and Zhang, X.D. (2015), "Health monitoring sensor placement optimization for Canton Tower using virus monkey algorithm", *Smart Struct. Syst., Int. J..*, **15**(5), 1373-1392. https://doi.org/10.12989/sss.2015.15.5.1373

Yi, T.H., Li, H.N. and Wang, C.W. (2016), "Multiaxial sensor placement optimization in structural health monitoring using distributed wolf algorithm", *Struct. Control. Hlth.*, **23**(4), 719-734. https://doi.org/10.1002/stc.1806

Yildizdan, G. and Baykan, Ö.K. (2020), "A novel modified bat algorithm hybridizing by differential evolution algorithm", *Expert Syst. Appl.*, **141**, 112949. https://doi.org/10.1016/j.eswa.2019.112949

Zhang, X.W., Gao, R.X., Yan, R.Q., Chen, X.F., Sun, C. and Yang, Z.B. (2016), "Multivariable wavelet finite element-based vibration model for quantitative crack identification by using particle swarm optimization", *J. Sound Vib.*, **375**, 200-216. https://doi.org/10.1016/j.jsv.2016.04.018

Zhou, L., Wu, S.Y. and Yang, J.N. (2008), "Experimental Study of an Adaptive Extended Kalman Filter for Structural Damage Identification", *J. Infrastruct. Syst.*, **14**(1), 42-51. https://doi.org/10.1061/(ASCE)1076-0342(2008)14:1(42)

BS